Electronic Supplementary Material (ESI) for ChemComm.

Supporting Information

Self-Assembled NIR Nanovesicles for Long-Term Photoacoustic Imaging *In Vivo*

Hong-Wei An,[a,b] Sheng-Lin Qiao,[a,b] Chun-Yuan Hou,[a] Yao-Xin Lin,[a,b] Li-Li Li,[a] Han-Yi Xie,[a] Yi Wang,[a,b] Lei Wang*,[a] and Hao Wang*,[a]

[a] *CAS Key Laboratory for Biological Effects of Nanomaterials and Nanosafety, National Center for Nanoscience and Technology (NCNST), No. 11 Beiyitiao, Zhongguancun, Beijing, China. E-mail: wanghao@nanoctr.cn*

[b] *University of Chinese Academy of Science (UCAS), No. 19A Yuquan Road, Beijing, China*

Table of Contents

1. Materials and methods

Chemicals and reagents: All reagents and solvents for organic synthesis were purchased from commercially available sources and used without further purification unless otherwise stated. DMEM medium, phosphate-buffered saline (PBS), and fetal bovine serum (FBS) were obtained from HyClone/Thermo fisher (Beijing, China). MCF-7 cell line was purchased from Cell Culture Center of Institute of Basic Medical Sciences, Chinese Academy of Medical Sciences (Beijing, China). Cell counting kit assay (CCK-8) was obtained from Beyotime Institute of Biotechnology (Shanghai, China). Dichloromethane (DCM) and N,N-dimethylformamide (DMF) were distilled over CaH_2 and stored under Ar. Silica gel (200-300 mesh) was used for column chromatography.

NMR spectroscopy: ^{1}H NMR were recorded at 298 K on a Bruker Advance 400M (400 MHz) spectrometer using $CDCl_3$ as solvent and tetramethylsilane (TMS) as an internal standard for the calibration of chemical shifts.

Mass spectrometry (MS) measurement: ESI mass spectra were measured with a Bruker APEX IV Fourier Transform Ion Cyclotron Resonance Mass Spectrometer. Microflex LRF MALDI-TOF was used to determine the molecular mass.

UV/Vis spectroscopy: UV/Vis absorption spectra were recorded on a Shimadzu 2600 UV/Vis spectrophotometer. The solvents for spectroscopic studies were spectroscopic grade and used as received. The spectra were recorded in quartz glass cuvettes and the extinction coefficients were calculated according to Lambert-Beer's law.

Fluorescence spectroscopy: Fluorescence spectroscopic studies were performed on a F-280 spectrofluorometer. The fluorescence quantum yield of monomeric **BP-Cy** was determined using the following equation according to the literature[1]: $\Phi_{F(x)} = (A_s/A_x)(F_x/F_s)(n_x/n_s)^2\Phi_{F(s)}$, where $\Phi_{F(x)}$ is the fluorescence quantum yield, A is the absorbance at the excitation

wavelength, *F* is the area under the corrected emission spectrum, and *n* is the refractive index of the solvents used. Subscripts "s" and "x" refer to the standard and to the unknown, respectively. ICG in methanol ($\Phi_{F(s)}$ = 0.078) was used as a reference.[2] The calculation performed by using above equation obtained quantum yields of **BP-Cy** in different solvents.

Transmission electron microscopy (TEM): The measurements were performed on a Tecnai G2 20 S-TWIN electron microscope operating at an acceleration voltage of 200 KV. For the observation of aggregates, a drop of sample solutions was placed on carbon-coated copper grids. The surface-deposited nanoparticles were negatively stained with 2% uranyl acetate for 40 s before the TEM studies.

Atomic force microscope (AFM): Morphology of the **BP-Cy** aggregation was characterized by using AFM on mica surfaces. The vesicle solution was drop cast on freshly cleaved mica surface at room temperature for 20 min. then the excessive solutions were withdrawn from the mica surface followed by nitrogen gas dry prior to AFM observations. AFM experiments were performed under ambient conditions using silicon cantilevers with nominal resonance frequency of 330 kHz in tapping mode on a Dimension 3100 system (Bruker Nano, USA).

Scanning electron microscope (SEM): The morphologies of **BP-Cy** aggregates were directly examined using scanning electron microscope. The studies were carried out on a Tecnai G2 F20 U-TWIN high-resolution electron microscope operating at an accelerating voltage of 500 KeV. The SEM samples were prepared by performing drop-coating of **BP-Cy** aggregates solutions onto silicon wafer. After contacting the droplets with silicon wafer for 5 minutes, an excess amount of droplets were removed by filter papers. Subsequently, the aggregates were coated by gold before scanning.

Vesicle preparation: Solvent-switch method was used to prepare **BP-Cy** vesicles. For a typical solvent-switch preparation, **BP-Cy** (weight of 0.2 mg) was dissolved in DMSO (10 μL),

and then deionized water (2 mL) was slowly injected into the above solution. The sample solution stayed under ambient conditions for several days before TEM measurement.

Light-thermo transformation: The 100 μL solution of **BP-Cy** and ICG was irradiation under the laser in wavelength 790 nm (490 mW) with an irradiated diameter of 2 mm. The temperature was recorded through thermal imaging system.

Hemolysis assay: The hemolytic activity of **BP-Cy** aggregates was investigated according to Fischer et al.[3]. Blood was collected in heparinized tubes from BALB/c mice followed by centrifugation at 3000 rpm for 10 min. Erythrocytes were then washed three times with cold phosphate saline buffer (PBS, pH 7.4) by centrifugation at 3000 rpm for 10 min and resuspended in the same buffer to a final cell concentration of 20% (v/v). This suspension can be kept at 4 °C for several days. **BP-Cy** aggregate solutions of different concentrations, also prepared in the PBS buffer, were added to the erythrocytes (final concentration 2%) and were incubated for 60 min at 37 °C in a shaking water bath. The release of hemoglobin is assessed by centrifugation (3000 rpm for 10 min) and spectrophotometric determination of the absorbance of the supernatant at 540 nm. Complete hemolysis was achieved using 0.2% Triton X-100 yielding the 100% control value. The experiments were run in triplicate. The percentage of hemolysis was calculated as follows:

Hemolysis percentage = $(A_S - A_N) / (A_P - A_N) \times 100$,

where A_S, A_P and A_N are the absorbance of the sample, positive control and negative control, respectively.

PA imaging of BP-Cy aggregates in cells: MCF-7 cells were grown in DMEM containing 10% FBS and 1% penicillin-streptomycin in a humidified atmosphere with 5% CO_2. The cells (plated at high density, 8 million cells in a 10 cm dish at 100% confluence) were incubated for 2 h with 10 μM **BP-Cy** aggregates and ICG in 37 °C, respectively. After a PA image was

taken at the end of incubation (referred to as the end of the first generation), 50% of the cells in the completely filled Petri dish were transferred to a new dish with fresh growth medium. Another image was taken after 36 h in the half-filled Petri dish, i.e., the end of the second generation. The living cells were further incubated for another 36 h to the end of the third generation. This process was repeated to proceed to the 7th generation.

Cell imaging in agarose for long time: MCF-7 cells were grown in DMEM containing 10% FBS and 1% penicillin-streptomycin in a humidified atmosphere with 5% CO_2. The cells (plated at high density, 8 million cells in a 10 cm dish at 100% confluence) were incubated for 2 h with 10 μM **BP-Cy** aggregates and ICG in 37 °C, respectively. Subsequently, the cells were washed with cold PBS three times and then harvested by trypsin. 8 million cells in PBS were mixed 1:1 with 1% ultrapure agarose (melting point 65 °C) in PBS, and then were added to the wells of the agarose gel photon made in advance. Afterward the wells were covered with an additional layer of warm agarose (60 °C), cooled at room temperature. PA imaging was collected by using a PA instrument (MSOT 128 Multi-Spectral Optoacoustic Tomography) with 790 nm laser excitation for different time intervals.

In vivo PA imaging: The tumor xenografted mice were purchased from Department of Laboratory Animal Science, Peking University Health Science Center, and all animal experiments were conducted by its center. MCF-7 cells (5×10^6) in PBS (100 μL) solution were subcutaneously injected into the right flank of the mice. The initial body weight of mice was about 17-18 g. After three weeks of tumor formation, **BP-Cy** aggregates (20 μM, 200 μL) dispersed into PBS was intravenous injected into mice through tail vein. Tumor xenografted mice were treated with ICG by using the same condition as controls. After injection, the mice were scanned with MOST (mode: MOST 128, excitation wavelength at 700-850 nm at

different time intervals. All animal experiments were performed in compliance with guidelines set by the Institutional Animal Care and Use Committee (IACUC), SingHealth.

Cell cytotoxicity assay: MCF-7 cells were cultured as above mentioned. MCF-7 cells were seeded at a density of 1×10^4 cells/well in a 96-well plate. After 24 h incubation, MCF-7 cells were treated with **BP-Cy** aggregates at serial concentrations (1, 2, 4, 8, 10, 20 μM) for 24 h. Then the medium was removed and cells were washed with PBS twice. Cell viability was determined by CCK-8 assay, and data were expressed as mean ± standard deviation (SD) for at least three independent experiments.

2. **Synthesis and characterization**

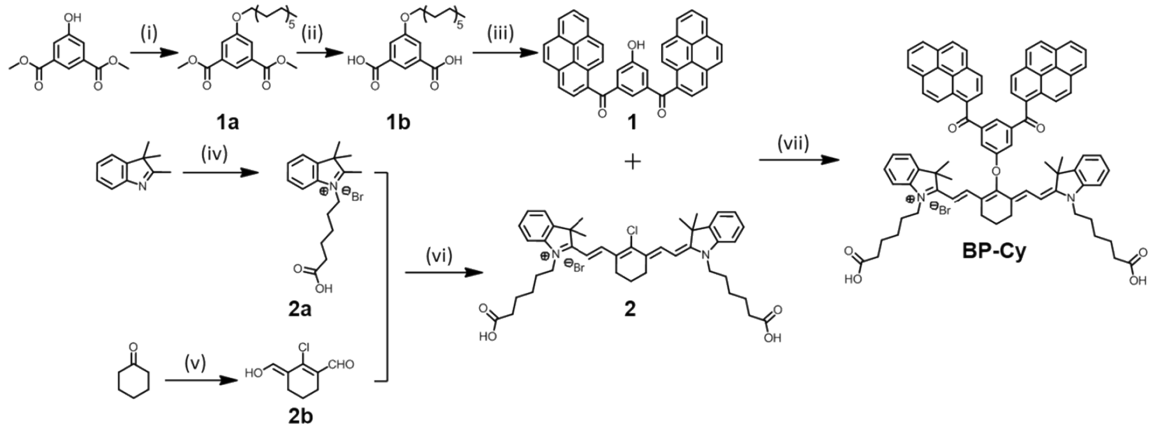

Scheme S1. Synthetic route of compound **BP-Cy**. Reagents and conditions: (i) 1-bromododecane, K_2CO_3, acetone, 70 °C, 72 h; (ii) KOH, H_2O/EtOH, 80 °C, 48 h; (iii) $SOCl_2$, DMF, reflux 12 h; $AlCl_3$, CH_2Cl_2, 0°C-r. t., 12 h; (iv) 6-bromohexanoic acid, toluene, 100 °C, 20 h; (v) $POCl_3$, DCM, DMF, reflux 2 h; (vi) Acetic anhydride, sodium acetate, r. t., 3 h; (vii) NaH, DMF, r. t., 10 min.

Dimethyl 5-(dodecyloxy)isophthalate (**1a**)

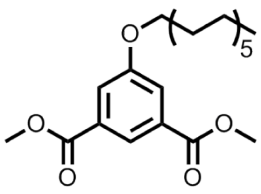

Dimethyl 5-hydroxyisophthalate (10.0 g, 47.6 mmol) , 1-bromododecane (14.2 g, 57.1 mmol) and K_2CO_3 (9.8 g, 71.4 mmol) were dissolved in dry acetone (100 mL). The reaction mixture was refluxed for 48 h. Then the solvents were removed under vacuum and the residue was dissolved in methylene chloride (300 mL), washed with saturated brine (3 × 150 mL). The extract was dried over anhydrous Na_2SO_4 to evaporate the solvent to afford white solid, 18.0 g, yield: 99%. The solid was kept in a refrigerator without further purification for next step reaction directly.

5-(dodecyloxy)isophthalic acid (**1b**)

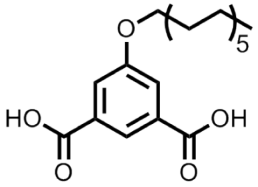

Compound **1a** (18.0 g, 47.6 mmol) and KOH (6.7 g, 114.2 mmol) were dissolved in H_2O/EtOH (v:v = 2:1, 225 mL). The reaction mixture was refluxed for 48 h and cooled down to room temperature. The reaction mixture was added with 1N HCl until the pH to 3. White solid were obtained by filtration (15.0 g, yield: 90%). The solid was kept in a refrigerator without further purification for next step reaction directly.

(5-hydroxy-1,3-phenylene) bis (pyren-1-ylmethanone) (**1**)

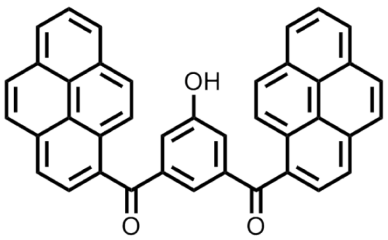

Compound **1b** (1.0 g, 2.9 mmol), 10 mL of $SOCl_2$ and 0.2 mL DMF were put into a 50 mL, round bottomed flask under N_2 atmosphere and the mixture was refluxed for 12 h. The solvent was removed in vacuum. The residue and pyrene (1.4 g, 7.0 mmol) were dissolved in

30 mL dry methylene chloride, and the mixture was cooled to 0 °C. After the portion-wise addition of $AlCl_3$ (1.0 g, 7.0 mmol), the mixture was allowed to react overnight at room temperature. The mixture was poured into ice-water and stirred until the color of the organic phase turned from black to yellow. The aqueous phase was extracted with methylene chloride, the combined organic phase was dried with $MgSO_4$ and the solvent was evaporated. The residue was purified through the silica gel column chromatography rinsed by a mixture eluent of methylene chloride/ethyl acetate with the gradient from 100: 0 to 95: 5 (v:v). The solvent was evaporated to give yellow solid product, 0.9 g, yield: 56%. ^{1}H NMR (400 MHz, $CDCl_3$, 298 K, TMS): δ = 8.38 (d, J = 10.0 Hz, 2H, ArH); 8.27-8.23 (m, 4H, ArH); 8.16-8.12 (m, 4H, ArH); 8.09-7.97 (m, 8H, ArH); 7.78 (s, 1H, ArH); 7.67 (s, 2H, ArH). MS (MALDI-TOF) calculated for $C_{40}H_{22}O_3$, 550.15 m/z, found 550.05.

1-(5-carboxypentyl)-2,3,3-trimethyl-3H-indol-1-ium bromide (**2a**)

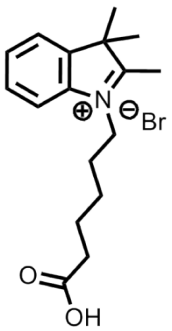

2,3,3-trimethylindolenine (3.2 mL, 20.0 mmol) and 6-bromohexanoic acid (3.9 g, 20.0 mmol) were dissolved in toluene (5 mL). The mixture was heated under reflux for 24 h. Then the reaction mixture was cooled to room temperature and filtered. The precipitate was washed with ether (3 × 10 mL) to obtain the pink crystals (6.4 g, yield: 90%). The crystals were kept in a refrigerator without further purification for next step reaction directly

(E)-2-chloro-3-(hydroxymethylene)cyclohex-1-enecarbaldehyde (**2b**)

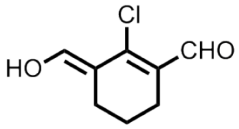

The dimethylformamide (40 mL) and methylene chloride (40 mL) were chilled in an ice bath, and then 19 mL of phosphorus oxychloride dissolved in 18 mL of methylene chloride was added dropwise with stirring, followed by 5 g of cyclohexanone. The solution was refluxed for 3 h, cooled, poured onto 100 g of ice, and allowed to stand overnight. The yellow solid was crystallized from a small volume of acetone cooled with ice. The yellow solid was collected and dried in vacuum (6.3 g, yield: 71%). The solid was kept in a refrigerator without further purification for next step reaction directly.

1-(5-carboxypentyl)-2-((E)-2-((E)-3-((E)-2-(1-(5-carboxypentyl)-3,3-dimethylindolin-2-ylidene)ethylidene)-2-chlorocyclohex-1-en-1-yl)vinyl)-3,3-dimethyl-3H-indol-1-ium bromide (**2**)

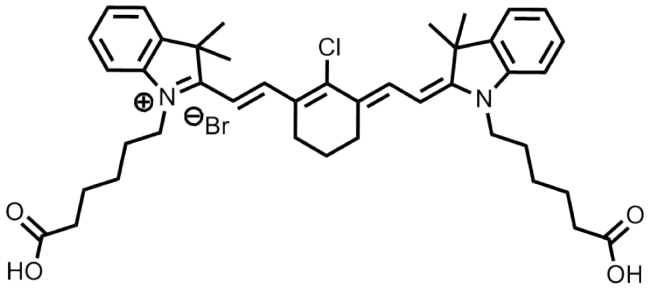

Compound **2a** (354.0 mg, 1.0 mmol), compound **2b** (78.5 mg, 0.5 mmol) and sodium acetate (41.0 mg) were dissolved in acetic anhydride (10 mL). The mixture was stirred at room temperature for 3 h. Then the solvents were poured in 200 mL diethyl ether to remove acetic anhydride by filter. The solid was washed with saturated brine (20 mL). The extracted with methylene chloride (3 × 50 mL). The extract was dried over anhydrous Na_2SO_4 to evaporate the solvent and afford dark green solid. The solid was purified through the silica gel column chromatography rinsed by a mixture eluent of methylene chloride/methanol with the gradient from 99:1 to 95:5 (v:v) to give a solid product, 240.5 mg, yield: 65%. ^1H

NMR (400 MHz, $CDCl_3$, 298 K, TMS): δ = 8.36 (d, *J* = 14 Hz, 2H, CH); 7.42-3.67 (m, 4H, ArH); 7.26-7.18 (m, 4H, ArH); 6.21 (d, *J* = 14 Hz, 2H, CH); 4.14 (t, *J* = 7.2 Hz, 4H, NCH_2); 2.72 (s, 4H, CH_2CH); 2.49 (t, *J* = 6.4 Hz, 4H, CH_2CO); 2.02-1.99 (m, 2H, CH_2); 1.89-1.85 (m, 4H, CH_2); 1.78-1.75 (m, 4H, CH_2); 1.75 (s, 12H, CH_3); 1.59-1.52 (m, 4H, CH_2). MS (MALDI-TOF) calculated for $C_{42}H_{52}ClN_2O_4$, 683.36 m/z, found 682.89.

1-(5-carboxypentyl)-2-((E)-2-((E)-3-((E)-2-(1-(5-carboxypentyl)-3,3-dimethylindolin-2-ylidene)ethylidene)-2-(3,5-di(pyrene-1-carbonyl)phenoxy)cyclohex-1-en-1-yl)vinyl)-3,3-dimethyl-3H-indol-1-ium bromide (**BP-Cy**)

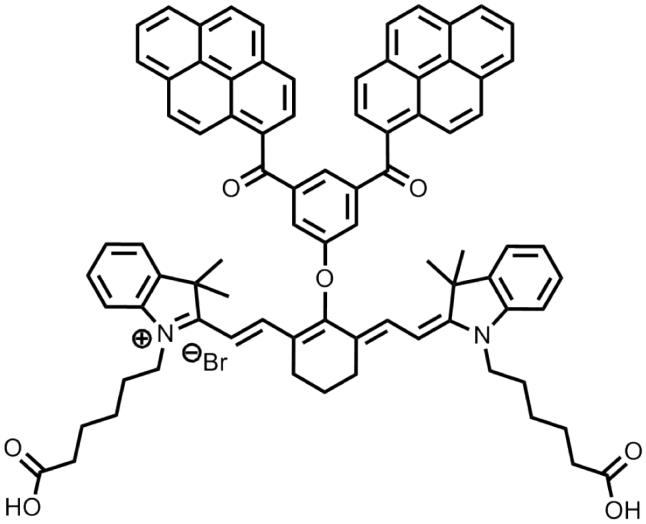

Compound **1** (22.0 mg, 0.039 mmol) and NaH (1.6 mg, 0.039 mmol) were dissolved in 5 mL dry DMF, and stirred at room temperature for 0.5 h, then compound **2** (20.0 mg, 0.026 mmol) was added into above solution. The solution was stirred at room temperature absent from light for another 10 minutes, then added 1 mL methylene chloride and with 1N HCl until the pH to 5-6. The mixture was poured into 100 mL ether to remove supernate by filter. The crude product was further purified by silica gel column chromatography rinsed by a mixture eluent of methylene chloride /methanol with the gradient from 95:5 to 80:20 (v:v) to give 23.3 mg of final product (yield: 69%). ^{1}H NMR (400 MHz, $CDCl_3$, 298K, TMS): δ = 8.28 (d, *J* = 9.6 Hz, 2H, CH); 8.21 (d, *J* = 7.6 Hz, 2H, ArH); 8.14 (d, *J* = 7.6 Hz, 2H, ArH); 8.09 (d, *J* = 8.8 Hz,

2H, ArH); 8.02-7.98 (m, 4H, ArH); 7.92-7.89 (m, 8H, ArH); 7.85 (s, 1H, ArH); 7.81 (s, 1H, ArH); 7.78 (s, 1H, ArH); 7.31 (m, 2H, ArH); 7.15 (m, 4H, ArH); 7.07 (d, *J* =8.0, 2H, ArH); 5.98 (d, *J* = 14 Hz, 2H, CH); 3.88 (s, 4H, CH_2N); 2.52 (s, 4H, CH_2); 2.38 (t, *J* = 9.6, 4H, $COCH_2$); 1.76 (m, 10H, CH_2), 1.50 (m, 4H, CH_2); 1.41 (s, 12H, CH_3). MS (MALDI-TOF) calculated for $C_{82}H_{73}N_2O_7$, 1197.5418 m/z, found 1197.07. HRMS (ESI positive) calculated for $C_{82}H_{73}N_2O_7$, 1197.5418 m/z, found 1197.5391.

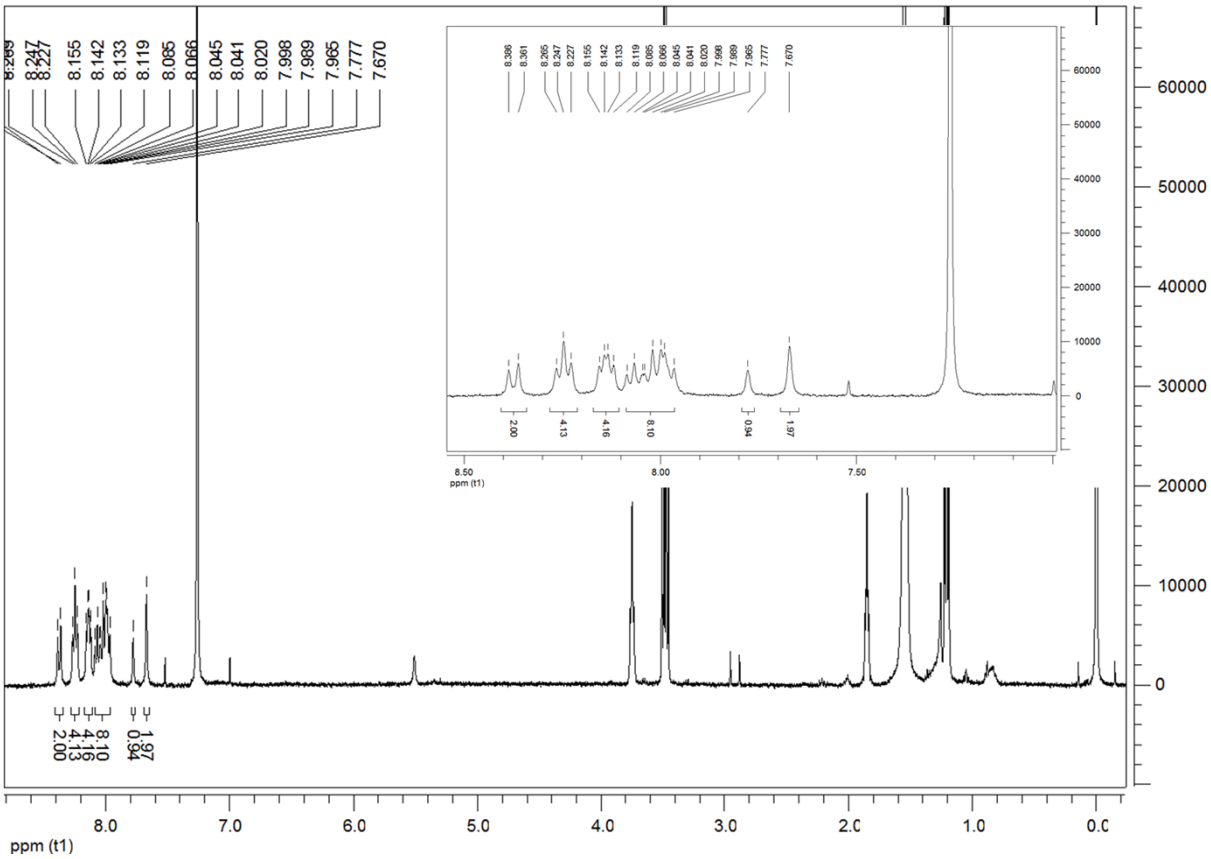

Figure S1. ^{1}H NMR spectrum of compound **1** in $CDCl_3$.

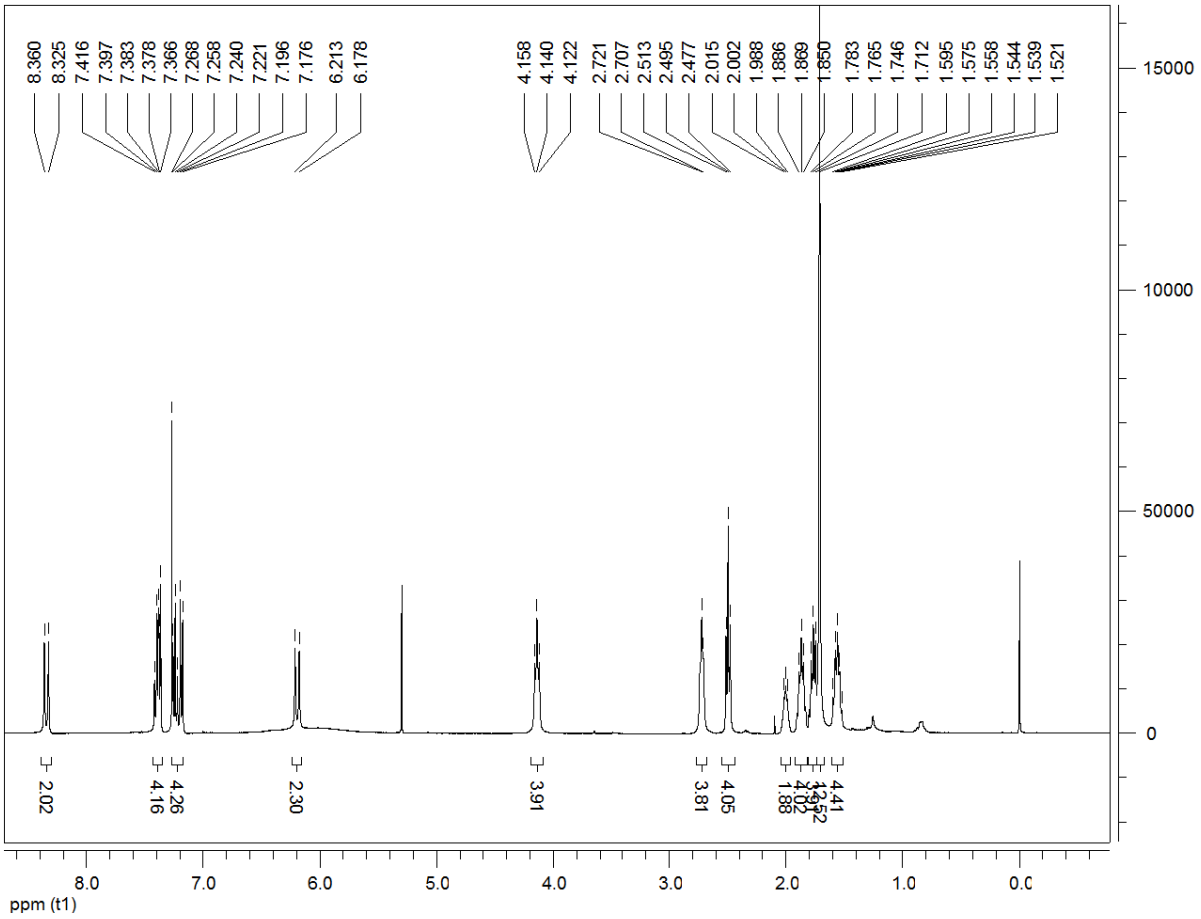

Figure S2. ^{1}H NMR spectrum of compound **2** in $CDCl_3$.

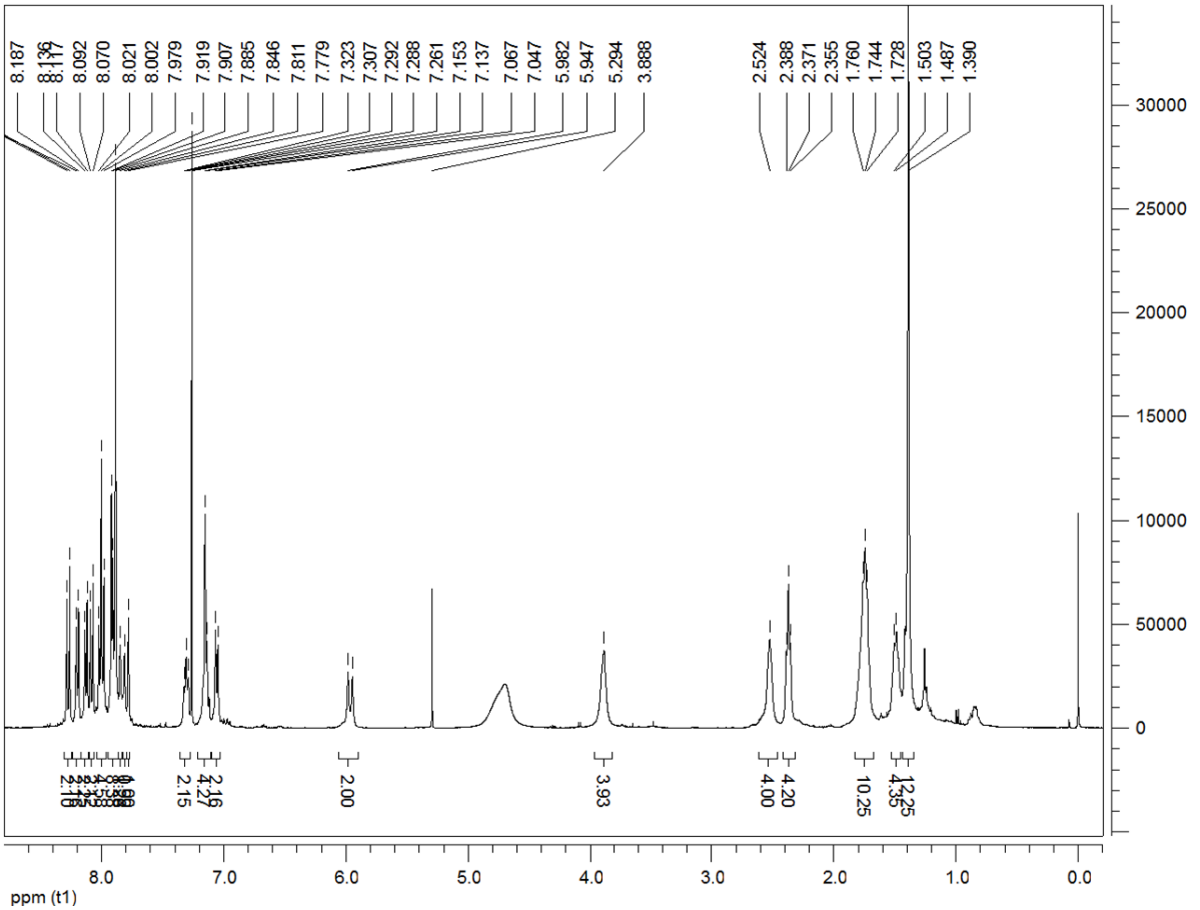

Figure S3. ^{1}H NMR spectrum of compound **BP-Cy** in $CDCl_3$.

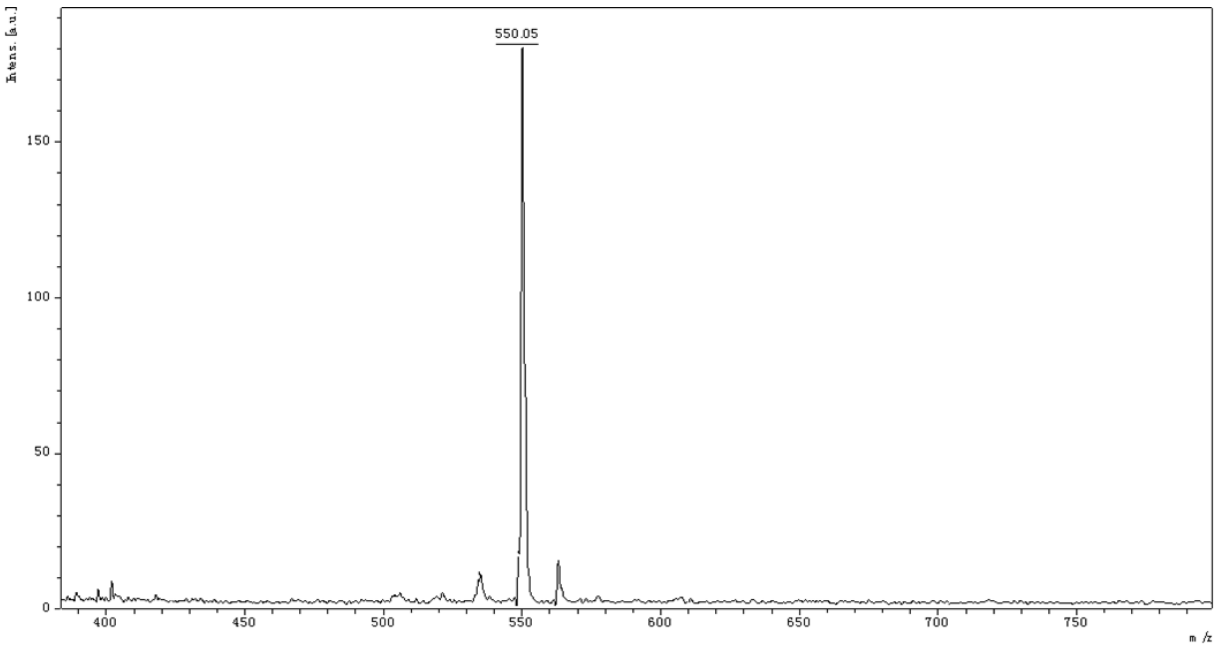

Figure S4. The MALDI-TOF spectrum of compound **1**.

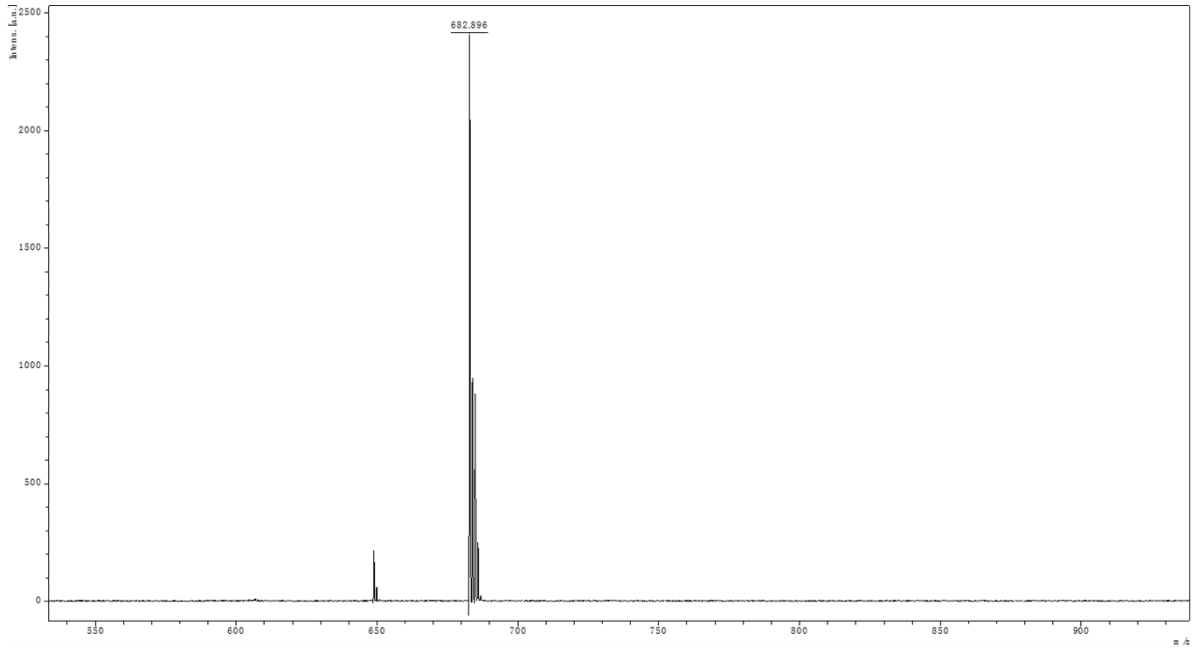

Figure S5. The MALDI-TOF spectrum of compound **2**.

Peking University Mass Spectrometry Sample Analysis Report

Analysis Info

Analysis Name	14080181_20140813_000008.d	Acquisition Date	8/13/2014 12:01:31 PM
Sample	H-59	Instrument	Bruker Apex IV FTMS
Comment	ESI Positive	Operator	Peking University

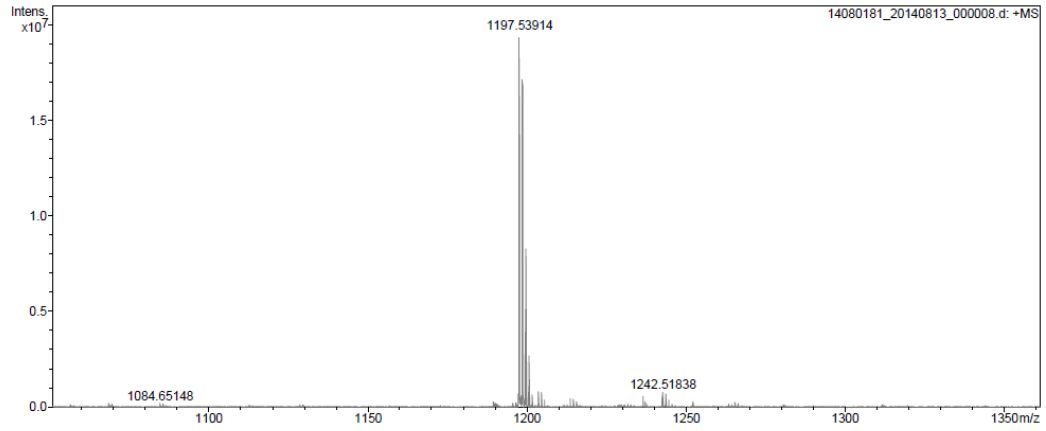

Meas. m/z	I	Formula	m/z	err [mDa]	err [ppm]	mSigma	rdb	e⁻ Conf	N-Rule
1197.53914	19582254	C 82 H 73 N 2 O 7	1197.54123	2.09	1.75	5.5	47.5	even	ok

Bruker Compass DataAnalysis 4.0 printed: 8/13/2014 12:02:33 PM Page 1 of 1

Figure S6. The HRMS-ESI spectrum of compound **BP-Cy**.

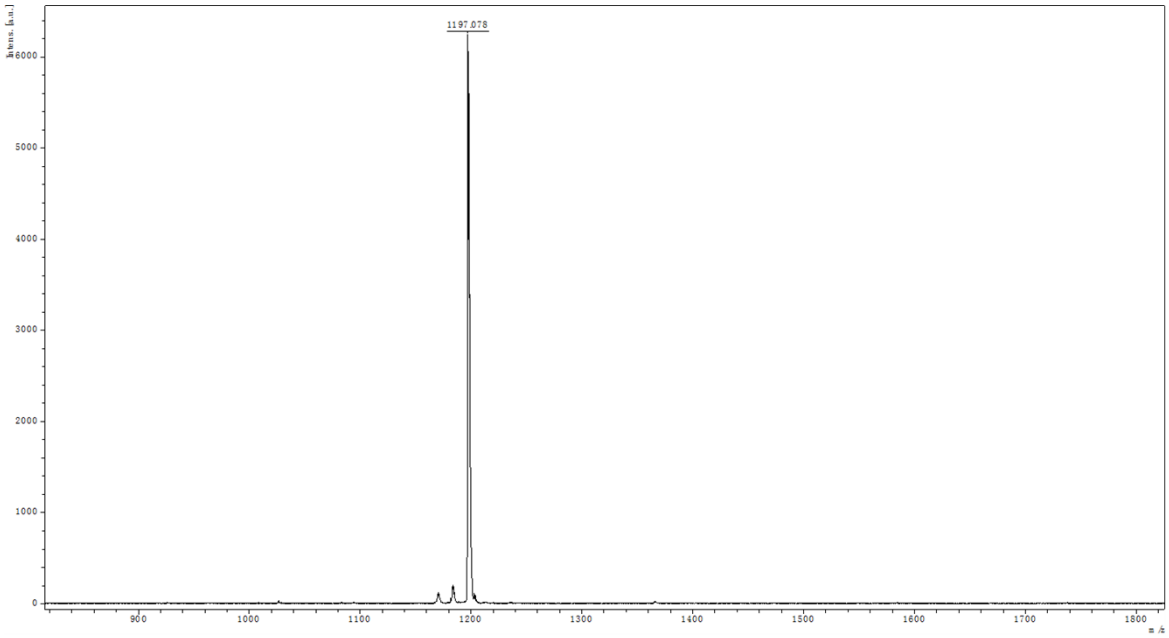

Figure S7. The MALDI-TOF spectrum of compound **BP-Cy**.

Table S1: Electronic absorption and fluorescence characteristics of **BP-Cy** in different solvents. The fluorescence quantum yields of **BP-Cy** were obtained in different solvent using **ICG** (methanol) as a reference standard (λ_{Ex} =785 nm).

Solvent	$\lambda^{[a]}_{max}$ (nm)	$\lambda^{[b]}_{em}$ (nm)	ε (M^{-1} cm^{-1})	Quantum Yield (%)
H_2O	787	-	59,000	0.07
DMSO	790	818	198,000	16.46±0.46
MeOH	780	806	279,000	12.95±0.43
DCM	790	812	258,000	24.56±0.33
MCH	798	-	52,000	0.21±0.02

[a] UV/Vis absorption maximum in different solvents. [b] The fluorescence emission maximum in different solvents with excitation at 785 nm.

3. UV-vis and fluorescence spectroscopic studies of aggregation

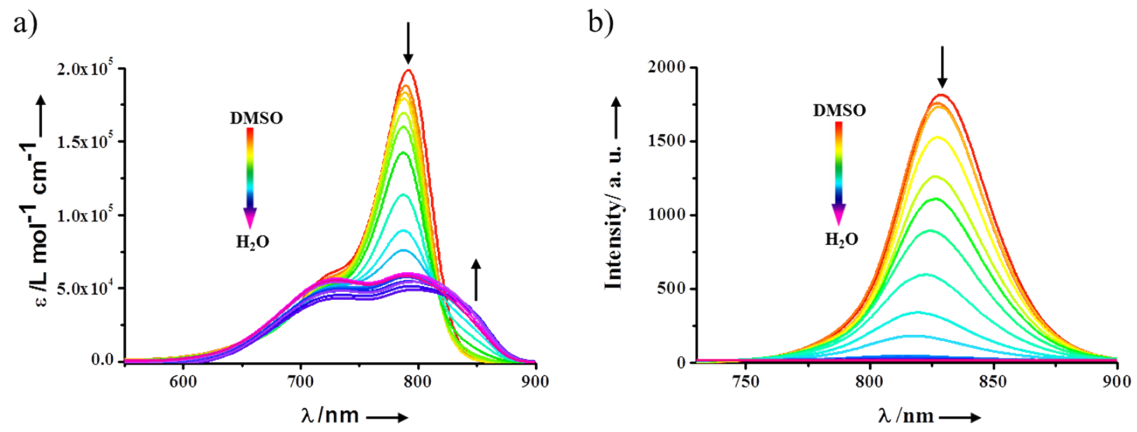

Figure S8. a) UV-vis and b) fluorescence emission of **BP-Cy** (10 μM) in DMSO/H_2O mixtures from 100:0 to 1:99 (v:v) at 25 °C. Arrows indicate spectral changes upon increase of water content.

4. The size and morphology of BP-Cy aggregates

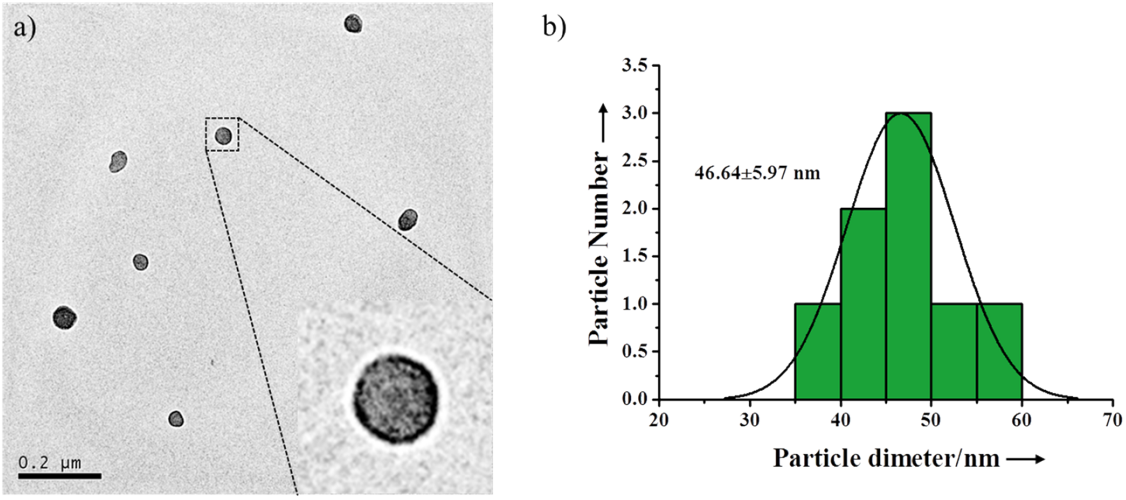

Figure S9. a) TEM images of **BP-Cy** aggregates with negative staining using uranyl acetate of vesicles, showing vesicular morphology. b) The size distribution of **BP-Cy** aggregates obtained from TEM imaging.

5. The stability of BP-Cy aggregates

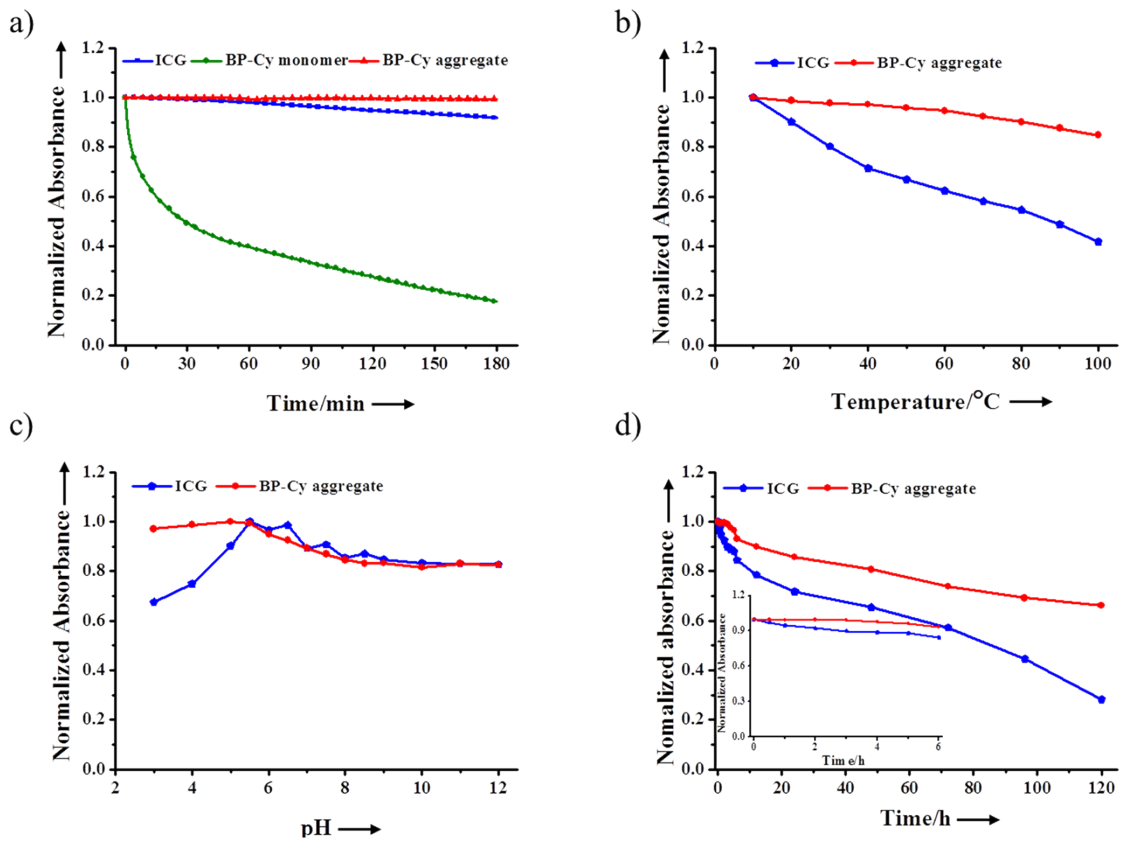

Figure S10 a) Photostability of ICG, **BP-Cy** monomer and **BP-Cy** aggregate under illumination lamp of UV2600 at 790nm. b) The thermal stability of ICG and **BP-Cy** aggregate at different temperature upon heating. c) pH stability of ICG and **BP-Cy** aggregate in buffer solution (PBS) with different pH value. d) The time-dependent stability of ICG and **BP-Cy** aggregate in cell culture medium (DMEM containing 10% fetal bovine serum and 1% penicillin-streptomycin) at 37 °C. The concentration of ICG and and **BP-Cy** were 10 μM in these experiments.

Table S2: Percentage release of hemoglobin (mean±SD) of BALB/c mice red blood cells after 1 h incubation with different concentrations of **BP-Cy** aggregate at 37 °C (n=3).

Conc. (μmol/L)	**4**	**8**	**12**	**16**	**20**	**24**	**32**	**40**
BP-Cy aggregate	**0.71±0.69**	**0.57±1.50**	**0.71±0.75**	**0.57±0.12**	**0.57±0.81**	**0.43±0.21**	**1.21±0.44**	**1.85±0.96**

Conc. stands for concentration.

6. PA imaging *in vitro* and *in vivo* based on BP-Cy aggregates

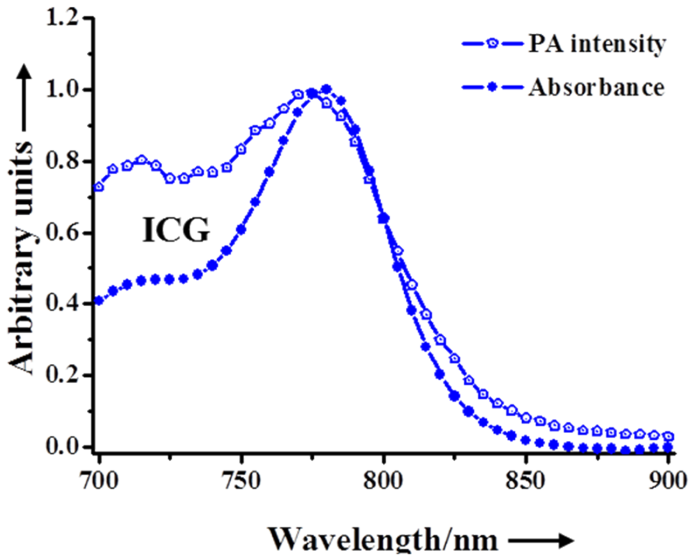

Figure S11. The normalized absorbance and PA intensity were a function of wavelength. The strong correlation between optical absorption and the PA effect is illustrated by the similarity in trend between the two graphs for each contrast agent, with a peak at around 790 nm.

The correlation of the PA signal: the equation of the PA signal proportionate to the local pressure rise as follow[4]:

$$p \propto \Gamma \eta \mu_a F \quad (1)$$

Where Γ was Grueneisen parameter (dimensionless), μ_a was the optical absorption coefficient (cm^{-1}), η was the thermal conversion efficiency, and F was the local optical fluence ($J \cdot cm^{-2}$).

According to the equation (1), the optical absorption coefficient and thermal conversion efficiency of different molcecular PA contrast agents (ICG and **BP-Cy** aggregates in our study) are main effects on the PA signals when the experiments were carried out at the same condition. The optical absorption coefficient of ICG and **BP-Cy** aggregates were 9.5×10^4 (Figure S10) and 5.9×10^4 $L\ M^{-1}\ cm^{-1}$ (Figure S7). The 1.6-fold PA intensities **BP-Cy** aggregates over ICG was ascrbed that the thermal conversion efficiency of **BP-Cy** aggregates should be

higher than that of ICG. Hence, the photothermal conversion experiment (Figure 2d) was carried out to confirm this assumption based on the equation 1. The thermal conversion efficiency η can be calculated by the following equation:

$$\eta = [hs (T_{max}-T_{envir.}) - Q_{dis}]/ I (1-10^{-Ab790}) \quad (2)$$

$$hs = m C_p / r'_s \quad (3)$$

$$r'_s = -Ln (\theta)/ t \quad (4)$$

$$\theta = (T-T_{envir})/(T_{max}-T_{envir.}) \quad (5)$$

Where T_{max} was the maximum temperature increase of the solution under irradiation time, T_{envir} was the temperature of the environment, Ab_{790} was the absorption of the compound at 790 nm, m was the mass of the solution, t was the irradiation time, I was the output power of the laser (490 mW), and r'_s was the slope of the line of time dependent -Ln (θ).[5] Q_{dis} was ignored due to the negligible baseline energy output. The calculated η value of **BP-Cy** aggregates is 9.2 times higher than that of ICG. The results displayed that the high thermal conversion efficiency **BP-Cy** nanovesicles contribute to the high PA intensity.

7. The cell viability of BP-Cy aggregates

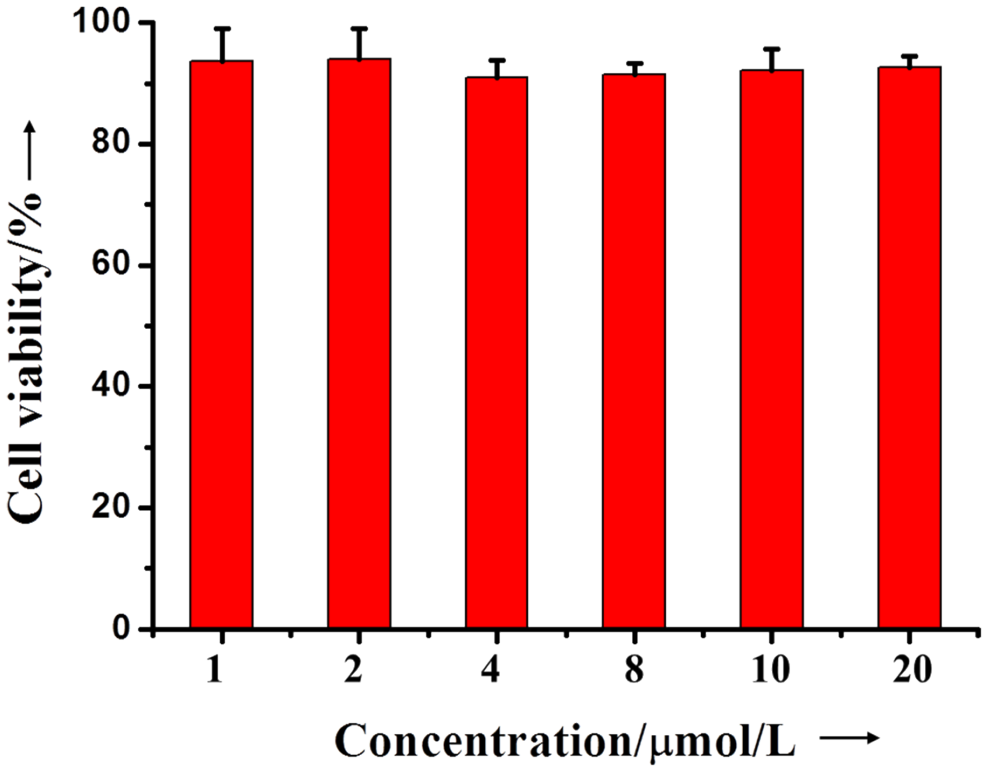

Figure S12. MCF-7 cell viability incubated with **BP-Cy** aggregates measured by the CCK-8 assay. Results are presented as the mean ± SD in triplicate.

8. Supporting references

1 S. Fery-Forgues, D. Lavabre, *J. Chem. Edu.* **1999**, *76*, 1260.
2 N. S. James, Y. Chen, P. Joshi, T. Y. Ohulchanskyy, M. Ethirajan, M. Henary, L. Strekowsk, R. K. Pandey, *Theranostics* **2013**, *3*, 692-702.
3 D. Fischer, Y.-X. Li, B. Ahlemeyer, J. Krieglstein, T. Kissel, *Biomaterials* **2003**, *24*, 1121-1131.
4 A. Danielli, C. P. Favazza, K. Maslov, L. V. Wang, *Appl. Phys. Lett.* **2010**, *97*, 163701.
5 Q. Tian, F. Jiang, R. Zou, Q. Liu, Z. Chen, M. Zhu, S. Yang, J. Wang, J. Wang, J. Hu, *ACS nano* **2011**, *5*, 9761-9771.